Applied Catalysis A, General 546 (2017) 111–121

Contents lists available at ScienceDirect

Applied Catalysis A, General

journal homepage: www.elsevier.com/locate/apcata

Feature Article

Effect of the size of Cu clusters on selectivity and activity of acetylene selective hydrogenation

Bo Zhao[a], Riguang Zhang[a,b,*], Zaixing Huang[b], Baojun Wang[a,*]

[a] Key Laboratory of Coal Science and Technology of Ministry of Education and Shanxi Province, Taiyuan University of Technology, Taiyuan 030024, Shanxi, PR China
[b] Department of Chemical and Petroleum Engineering, The University of Wyoming, Laramie, WY 82071, USA

ARTICLE INFO

Keywords:
Acetylene
Hydrogenation
Copper cluster
Size effect
Selectivity
Activity

ABSTRACT

In order to probe into the size effect of Cu catalyst on the selectivity and activity of ethylene formation in acetylene selective hydrogenation, different sizes of Cu catalysts including Cu_{13}, Cu_{38}, Cu_{55} clusters and the periodic Cu(111) surface have been employed to systematically investigate the selective hydrogenation of C_2H_2 using density functional theory calculations. The results show that the adsorption ability of C_2H_2 is stronger than that of C_2H_4 on different sizes of Cu catalysts, which is in favor of C_2H_2 activation and hydrogenation. On Cu_{13} and Cu_{38} clusters, C_2H_2 easily undergoes over-hydrogenation to form ethane *via* $CHCH_2$ and $CHCH_3$ intermediates, namely, both clusters exhibit a poor selectivity towards C_2H_4 formation. However, on Cu_{55} cluster, C_2H_2 is easily hydrogenated to form C_2H_4 *via* $CHCH_2$ intermediate, and C_2H_4 prefers desorption over its hydrogenation, suggesting that Cu_{55} cluster exhibits a good selectivity towards C_2H_4 formation. Further, the periodic Cu(111) surface regarded as the large Cu particle sizes has the same results with Cu_{55} cluster. Therefore, among different sizes of Cu cluster, the size of Cu cluster affects the preferred pathway of C_2H_2 selective hydrogenation, and alters the selectivity towards C_2H_4 formation; moreover, beginning with Cu_{55} cluster, Cu cluster is beneficial to C_2H_2 hydrogenation to C_2H_4. The activity of C_2H_4 formation follows the order of Cu(111) > Cu_{38} > Cu_{55} > > Cu_{13}, which corresponds to the *d*-band center of these catalysts. The identifications about the relationship of the intrinsic selectivity and activity with cluster size effect would provide a clue for designing highly-efficient Cu-based catalysts in C_2H_2 hydrogenation to C_2H_4.

1. Introduction

Ethylene (C_2H_4) from the decomposition of the higher hydrocarbons is widely used as a polymerization feed stock and an important intermediate in many industrial reactions. However, during the decomposition process of the higher hydrocarbons, about 0.1–1% of acetylene (C_2H_2) is produced, which can poison the downstream catalyst used for C_2H_4 polymerization, as a result, the quality of poly-ethylene production will also be affected due to the presence of C_2H_2 [1,2]. Thus, C_2H_2 hydrogenation to C_2H_4 in excess C_2H_4 feed becomes an important industrial process, and it is of great economic value to promote C_2H_2 hydrogenation to C_2H_4, but also purify C_2H_4 and increase its yield.

In order to remove C_2H_2 impurities from acetylene-ethylene feed, Pd-based catalysts have been widely used for C_2H_2 hydrogenation to C_2H_4 due to its high activity. However, Pd-based catalysts easily make C_2H_4 over-hydrogenation to ethane, which wastes the feed gas; as a result, Pd-based catalysts exhibit a poor selectivity towards C_2H_4 formation. Meanwhile, the high molecular weight oligomeric species such as oligomers from C_2H_2 polymerization can push away Pd particles from the support quickly to deactivate the catalyst [3]. Moreover, the hydride [4,5] and carbide [6–8] phases of metal Pd is easily formed to decrease C_2H_4 selectivity [9–16]. Thus, in order to achieve high C_2H_4 selectivity, one method is to add the second metal such as Cu into Pd, which exhibits a high alkene selectivity [17–21]; the other is to control the catalyst particle at a suitable size [22–25].

On the other hand, Kyriakou et al. [26] have explored a high-performance catalyst with doping a small quantities of Pd on Cu(111) surface, Cu becomes the dominant component while Pd acts as the promoter, this catalyst exhibits the higher C_2H_4 selectivity in C_2H_2 selective hydrogenation compared to the pure Cu or Pd alone. McCue et al. [27] have prepared Cu/Al_2O_3 catalyst modified with Pd for C_2H_2 selective hydrogenation, suggesting that Cu:Pd ratio of 50:1 presents a high selectivity and conversion (80% selectivity to C_2H_4 formation and more than 99% conversion at 363 K). These reported studies suggest that Cu-based catalysts also present high selectivity towards C_2H_2 selective hydrogenation to C_2H_4. Bridier et al. [28] develops a Cu-Ni-Fe

---

[*] Corresponding authors at: Key Laboratory of Coal Science and Technology of Ministry of Education and Shanxi Province, Taiyuan University of Technology, No. 79 Yingze West Street, Taiyuan, Shanxi, 030024, PR China.

E-mail addresses: zhangriguang@tyut.edu.cn (R. Zhang), wangbaojun@tyut.edu.cn, quantumtyut@126.com (B. Wang).

http://dx.doi.org/10.1016/j.apcata.2017.08.001
Received 22 February 2017; Received in revised form 6 July 2017; Accepted 1 August 2017

ternary catalysts with Cu as the base hydrogenation metal, which displayed an outstanding alkene selectivity, and Cu has an intrinsic activity for hydrogenation [17,18,29]. Further, previous studies about methanol decomposition also revealed that the effect of Cu size can alter the reaction pathway and product distribution [30]. However, to the best of our knowledge, few studies about the selective hydrogenation of C_2H_2 have been reported on Cu catalyst, moreover, the size effect of Cu catalyst on the catalytic activity and selectivity is still unclear, as a result, it is necessary to probe into the underlying mechanism of C_2H_2 selective hydrogenation at a molecular level on different sizes of Cu catalysts.

In this study, in order to probe into C_2H_2 selective hydrogenation on Cu catalyst and the size effect of Cu catalyst on the selectivity and activity, the underlying mechanism of C_2H_2 selective hydrogenation on different size of Cu clusters have been systematically investigated using density functional theory calculations. It is expected that the results can provide a good clue for designing the suitable particle size of highly-efficient Cu catalysts in C_2H_2 hydrogenation to C_2H_4.

2. Computational details

2.1. Computational method

All calculations have been performed using Dmol^3 program package in Materials Studio 5.5 [31,32], the generalized gradient approximation (GGA) with the Perdew-Wang exchange–correlation functional (PW91) was employed [33,34]. The double-numerical basis set with a polarization *d*-function (DNP) was selected. A 3 × 3 × 1 k-point sampling in the surface Brillouin zone was used for Cu(111) surface. 0.005 Hartree is set for the smearing value. An effective core potential (ECP) is used for Cu atoms and all-electron basis set is used for other atoms. Further, in order to search transition states of the reaction, the complete LST/QST approach have been used [35,36]. The transition state is confirmed by frequency analysis with only one imaginary frequency; moreover, TS confirmation has been used to confirm the transition state connected the reactant and product [37].

The adsorption energy of the species (E_{ads}) is calculated based on Eq. (1):

$$E_{ads} = E_{(adsorbate)} + E_{cluster/slab} - E_{total} \tag{1}$$

Where E_{total} is the energy of the total adsorbed system, $E_{(adsorbate)}$ is the energy of gas-phase molecule, and $E_{cluster/slab}$ is the energy of the clusters or slab.

In this study, the entropic effect has been considered for the adsorption and reaction. For the adsorption process, Gibbs free energy correction is calculated according to Eq. (2):

$$\Delta G_{Eads} = G_{(adsorbate)} + G_{cluster/slab} - G_{total} \tag{2}$$

Where $G_{(adsorbate)}$, $G_{cluster/slab}$ and G_{total} represent the Gibbs free energy of adsorbed molecules, clusters or slab, and the total energy of the adsorbed system.

The free adsorption energy at a definite temperature was defined as follows:

$$E_{ads,T} = E_{ads} + \Delta G_{Eads} \tag{3}$$

Similarly, the values of reaction energy (ΔH) and activation barrier (E_a) are defined as the Eqs. (3) and (4), respectively.

$$\Delta H = E_P - E_R + \Delta G \tag{4}$$

$$E_a = E_{TS} - E_R + \Delta G \tag{5}$$

Where E_P, E_R, *and* E_{TS} represent the total energies of the adsorbed reactant, product and the transition state on Cu cluster or slab, respectively, ΔG is the value of Gibbs free energy correction.

On the other hand, in order to obtain more H atoms aiming at inhibiting acetylene polymerization to form oligomer [38], C_2H_2 selective hydrogenation over Cu-based catalyst required a high operating temperature (> 473 K) under the experimental condition [28,39], the temperature is set to be 525 K. Meanwhile, previous studies have reported that PdCu catalyst exhibits a good activity and selectivity towards C_2H_2 hydrogenation to C_2H_4 at low temperatures [26,27], the temperature at 425 K is also examined. Further, previous studies [27] have shown that the higher H_2:C_2H_2 ratio (10:1) can reduce the oligomer formation by approximately 90% with ethane selectivity remaining around 10%, as a result, 10 atm was set for the total pressure, and 0.1, 1 and 8.9 atm correspond to the partial pressures of C_2H_2, H_2 and C_2H_4, respectively, which is close to the experimental conditions. Thus, this study only focuses on the selectivity of C_2H_4 formation in C_2H_2 selective hydrogenation on different sizes of Cu catalysts.

2.2. Surface model

For Cu clusters, there exist many isomers where cluster isomers numbers increases rapidly with the increasing of the cluster size, and it is an important factor to keep the cluster structural stability [40]. In this study, Cu_{13}, Cu_{38} and Cu_{55} nanoparticles with the corresponding diameters of 4.9, 7.6 and 9.8 Å are selected to probe into the effect of Cu cluster size on C_2H_2 selective hydrogenation. In addition, the periodic Cu(111) surface is regarded as the larger particle. Fig. 1 represents the most stable configurations of Cu_{13}, Cu_{38}, Cu_{55}, Cu_{147} clusters, and Cu (111) surface.

Cu_{13} cluster is the icosahedron structure including twenty (111) surfaces [41–48], and it is a core-shell structure with 12 atoms in outer shell and an atom in core shell; moreover, all shell atoms have the same coordination number 6, three adsorption sites exist: Top, Bridge and Hcp.

Cu_{38} cluster with the truncated octahedron structure is more stable than other isomers [45–53]. it has an outer shell of 32 atoms and a core shell of 6 octahedral atoms, moreover, the outer shell has 8 atoms at the center of (111) facet and 24 atoms on (100) facet. Due to different coordination number 6 and 9 for outer shell atoms, eight adsorption sites exist: Top I, Top II, Bridge I, Bridge II, Bridge III, Fcc, Hcp and Hollow. Top I and Top II are two Cu atom with different coordination number 6 at the vertex of (100) facet and 9 at the center of (111) facet. Other adsorption sites are formed on the basis of Top I and Top II sites.

For Cu_{55} cluster, the most stable structure is also the icosahedron structure with the high symmetry, which has been identified in the previous studies [45,47,54–56]. It has three shells with 42 atoms in the outer shell, 12 atoms in the second shell, and a Cu atom in the core. Obviously, the outer shell corresponds to (111) facet, and most surface atoms are located at the vertex and edge sites; the outer shell atoms have the coordination number 6 and 8, thus, six adsorption sites exist: Top I, Top II, Bridge I, Bridge II, Fcc and Hcp.

To exhibit a large Cu clusters, Cu_{147} cluster with a radius of 1.5 nm is selected. It is obvious that Cu_{13}, Cu_{55} and Cu_{147} are all the icosahedron structure, with the increasing of cluster size, the coordinated numbers of atoms on surface edge and vertex are keep at 6 and 8; Cu atoms with 9 coordination number appeared on Cu_{147} cluster. Moreover, with the size increased to 3.5 nm, the symmetry of metal clusters do not change, it still keep the quasicrystal icosahedral and decahedral structures, and the coordinated numbers of atoms on surface edge and vertex only keep in 6 and 8 [57]. As a result, the adsorption and reaction on the low-coordinated sites for large clusters should be similar to that on Cu_{55}, in order to probe into the effect of high coordination number Cu atoms, considering the time cost for the calculations on Cu_{147} cluster, Cu_{147} is not selected here replaced by Cu (111) surface with all Cu atoms coordination number 9, and it also be defined as a larger cluster. Cu(111) surface has four adsorption sites: Top, Bridge, Fcc and Hcp.

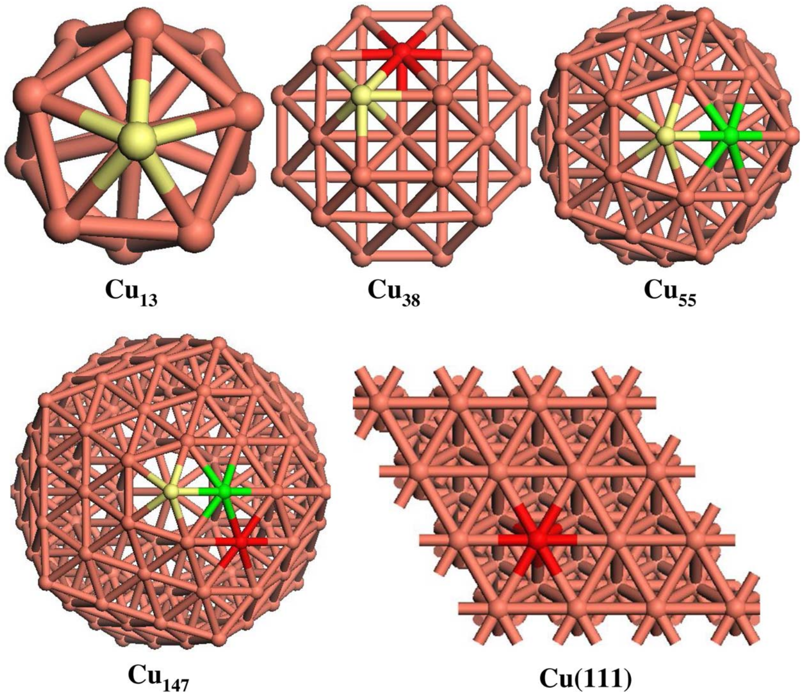

Fig. 1. The optimized structures for different sizes of Cu clusters and the Cu(111) surface. The yellow, blue and red atoms correspond to 6-, 8- and 9-coordination Cu atoms, respectively. (For interpretation of the references to colour in this figure legend, the reader is referred to the web version of this article.)

3. Results and discussion

3.1. *The proposed reaction pathway for C_2H_2 selective hydrogenation*

In order to probe into the catalytic performance of Cu catalyst towards C_2H_2 selective hydrogenation, it is necessary to understand the reaction mechanism of C_2H_2 selective hydrogenation, in this study, three possible pathways have been considered, as shown in Fig. 2, **Path I** is C_2H_2 hydrogenation to form C_2H_4 *via* C_2H_3 intermediate, followed by its desorption leading to gas phase C_2H_4; **Path II** is C_2H_2 hydrogenation to form C_2H_4 *via* C_2H_3 intermediate, followed by C_2H_4 hydrogenation to C_2H_5; **Path III** is C_2H_2 hydrogenation to C_2H_3, followed by its hydrogenation to C_2H_5 *via* $CHCH_3$ intermediate; C_2H_5 is easily hydrogenated to ethane. Thus, Paths II and III are disadvantageous to remove C_2H_2 impurities from acetylene-ethylene feed. Obviously, for our aim to purity ethylene feed, promoting Path I and/or suppressing Paths II and III is a better way to improve the selectivity of C_2H_2 hydrogenation to C_2H_4.

3.2. *Adsorption of all possible species in C_2H_2 selective hydrogenation*

Fig. 3 presents the stable adsorption configurations of all possible C_2H_2, C_2H_3, C_2H_4, $CHCH_3$ and C_2H_5 species in C_2H_2 selective hydrogenation. As mentioned in Introduction, there are about 0.1 ~ 1% C_2H_2 and 89% C_2H_4 in the feed gas under the experimental conditions of C_2H_2 selective hydrogenation, thus, only when the adsorption ability of C_2H_2 is much stronger than that of C_2H_4, the removal of trace C_2H_2 impurities from the large amount of C_2H_4 feed gas can be realized.

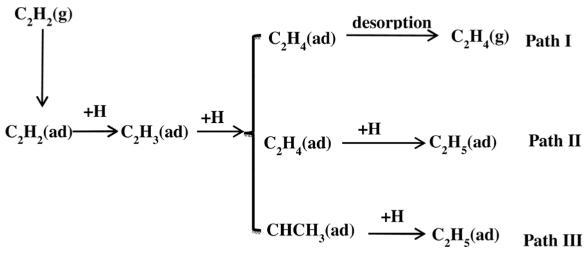

Fig. 2. Possible reaction pathways of C_2H_2 selective hydrogenation.

For C_2H_2 adsorption, our calculated results show that C_2H_2 in the gas phase has the values of d_{C-C} and d_{C-H} of 1.21 Å and 1.07 Å, respectively, which agree with the experimental values [58]. It can be seen that the free adsorption energies at 525 K are 248.4, 212.3, 160.6 and 140.4 kJ mol^{-1} on Cu_{13}, Cu_{38}, Cu_{55} clusters and the Cu(111) surface, respectively. On Cu_{38} and Cu_{55} clusters, it is adsorbed at the “4-fold diagonal hollow” site, which agree with that on Ni(111), Cu(111), Cu(100) surface [59,60]. On Cu_{13} cluster, C_2H_2 adsorbs at 3-fold hollow site via η^2-η^2 model, which is the same as that reported on Pd(111) [61].

For C_2H_4 adsorption, many studies [61,62] on Pt clusters and Pd surface suggests that the adsorption energy increases with the decreasing of surface atom coordination number. As shown in Fig. 3, C_2H_4 on three clusters interacts with a surface Cu atom with the coordination number 6. The corresponding free adsorption energies at 525 K are 133.6, 96.9, 115.6 and 70.6 kJ mol^{-1} on Cu_{13}, Cu_{38}, Cu_{55} clusters, and Cu(111) surface, respectively, indicating that the energetic trend for C_2H_4 adsorption over Cu clusters is correlated with the metal coordination number due to a reduced Pauli repulsion between ethylene-occupied molecular orbitals and the surface bands of the sites with low metal coordination number [62].

Above results show that the adsorption free energies of C_2H_2 is much larger by 114.8, 115.4, 45.0 and 69.8 kJ mol^{-1} than those of C_2H_4 on Cu_{13}, Cu_{38}, Cu_{55} and Cu(111), respectively. Namely, trace amounts of C_2H_2 impurities in the large amount of C_2H_4 feed gas is more favorable to adsorb than C_2H_4, which make C_2H_2 hydrogenation become possible on Cu catalyst.

3.3. *Acetylene hydrogenation on different cCu clusters and Cu(111) surface*

3.3.1. *The adsorption and dissociation of H_2*

Since the activation of H_2 is the source of adsorbed H atoms in the selective hydrogenation of C_2H_2, the adsorption and dissociation of H_2 is firstly examined on Cu_{13}, Cu_{55} clusters, and Cu(111) surface, the detailed results are presented in the Part 2 of Supplementary material.

The results show that on Cu_{13}, Cu_{55} clusters and Cu(111) surface, H_2 is the dissociative adsorption, the dissociation of H_2 is spontaneous to form the adsorbed H atoms, which can provide enough H atoms for the selective hydrogenation of C_2H_2. On the other hand, H_2 dominantly

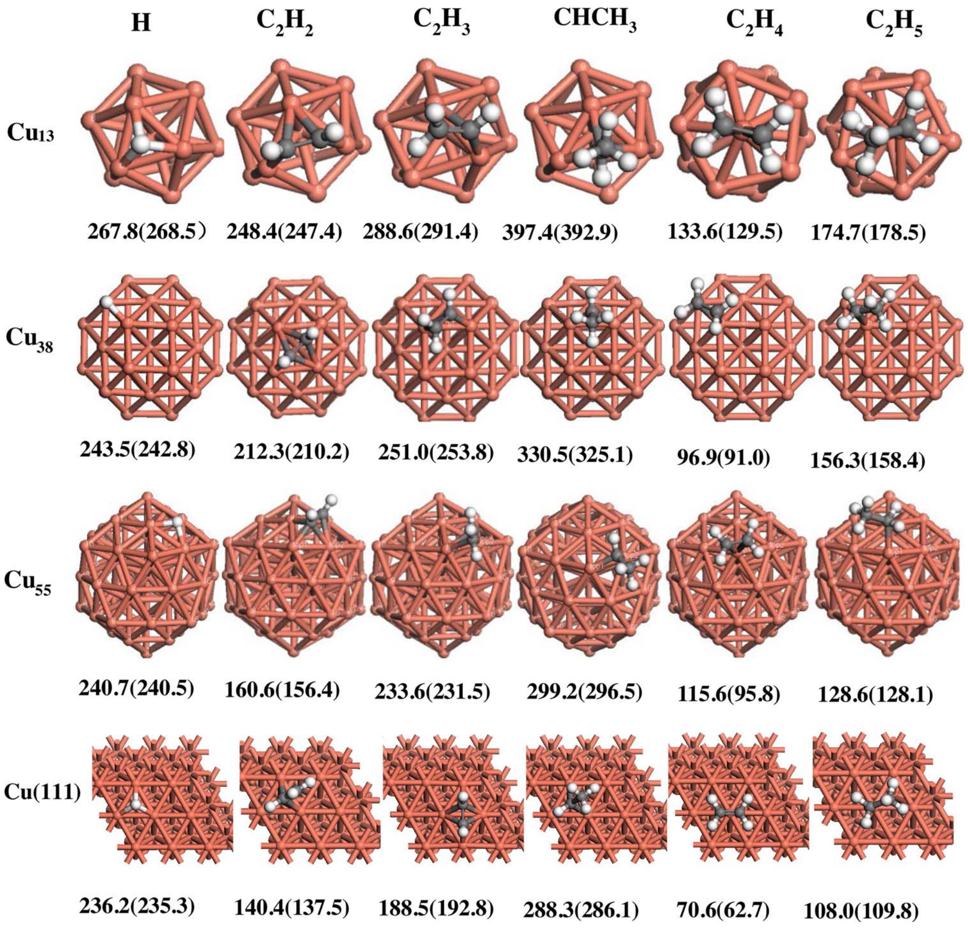

Fig. 3. The most stable adsorption configurations of C_2H_2, C_2H_3, C_2H_4, $CHCH_3$ and C_2H_5 species involved in C_2H_2 selective hydrogenation on different Cu clusters and Cu(111) surface together with the free adsorption energies at 525 K and those in parenthesis at 425 K. C, H, and Cu atoms are shown in the grey, white and orange balls, respectively. The energy unit is in kJ mol^{-1}. (For interpretation of the references to colour in this figure legend, the reader is referred to the web version of this article.)

exists in the form of molecular adsorption on Cu_{38} cluster; meanwhile, a small quantity of molecular adsorption H_2 also exist on Cu_{13}, Cu_{55} clusters and Cu(111) surface; the dissociation of molecular adsorption H_2 shows that the overall activation barrier of C_2H_2 hydrogenation to C_2H_4 is much higher than the dissociation barrier of H_2, suggesting that compare to C_2H_2 hydrogenation to C_2H_4, the dissociation of H_2 is more easier to occur, which can provide sufficient H atoms for the selective hydrogenation of C_2H_2 on Cu_{13}, Cu_{38}, Cu_{55} clusters and Cu(111) surface. Thus, in the selective hydrogenation of C_2H_2, the adsorption and dissociation of H_2 is easy to occur, and provide sufficient sources of H atoms on Cu_{13}, Cu_{38}, Cu_{55} clusters and Cu(111) surface.

3.3.2. The definitions of desorption barrier and C_2H_2 selectivity

Among three possible pathways of C_2H_2 selective hydrogenation, there is the common step of $C_2H_2 + H \rightarrow C_2H_3$. So, starting from C_2H_3 + H, the highest energy of each pathway from C_2H_3 to C_2H_5 is used to evaluate the favorable pathway. Moreover, previous studies [63] have shown that the desorption barrier is approximately equal to the absolute value of adsorption energy, as a result, the adsorption energy of C_2H_4 is used as its desorption barrier in Path I.

On the other hand, in order to evaluate the selectivity of C_2H_2 hydrogenation to C_2H_4, the difference between the hydrogenation barrier of C_2H_4 and its desorption barrier is used to estimate C_2H_4 selectivity, which is denoted according to the Eq. (6): $\triangle E_a = E_a - |E_{ads}|$, where E_a is the barrier of C_2H_4 hydrogenation, and E_{ads} is the corresponding adsorption energy of C_2H_4.

3.3.3. C_2H_2 hydrogenation on Cu_{13} cluster

As listed in Table 1, at 525 K, for the first step of C_2H_2 hydrogenation to the common intermediate C_2H_3, this elementary reaction

Table 1

The free activation barrier (E_a) and free reaction energy ($\triangle H$) of all possible elementary reactions on different Cu clusters, Cu(111) and PdCu(111) surfaces at 525 and 425 K.

Cu clusters	Elementary reactions	E_a/kJ mol^{-1}	$\triangle H$/kJ mol^{-1}
Cu_{13}	$C_2H_2 + H \rightarrow C_2H_3$	167.5 (184.8)	26.8 (31.4)
	$C_2H_3 + H \rightarrow IM$	156.2 (145.2)	−7.2 (−3.5)
	$IM \rightarrow C_2H_4$	27.7 (22.8)	10.8 (−0.5)
	$C_2H_3 + H \rightarrow CHCH_3$	107.4 (118.0)	12.2 (11.6)
	$C_2H_4 + H \rightarrow C_2H_5$	90.4 (88.3)	11.1 (17.8)
	$CHCH_3{-}C_2H_5$	129.7 (131.5)	2.5 (2.2)
Cu_{38}	$C_2H_2 + H \rightarrow C_2H_3$	76.3 (77.3)	−37.3 (−36.4)
	$C_2H_3 + H \rightarrow C_2H_4$	166.3 (162.9)	−28.2 (−28.6)
	$C_2H_3 + H \rightarrow CHCH_3$	121.3 (118.7)	18.7 (19.5)
	$C_2H_4 + H \rightarrow C_2H_5$	123.0 (118.7)	−27.2 (−24.9)
	$CHCH_3 + H \rightarrow C_2H_5$	140.8 (135.4)	−74.1 (−73.0)
Cu_{55}	$C_2H_2 + H \rightarrow C_2H_3$	137.0 (146.0)	−24.1 (−19.1)
	$C_2H_3 + H \rightarrow C_2H_4$	105.8 (112.8)	−77.1 (−64.4)
	$C_2H_3 + H \rightarrow CHCH_3$	154.4 (158.4)	22.6 (21.7)
	$C_2H_4 + H \rightarrow C_2H_5$	124.8 (128.2)	6.5 (4.7)
	$CHCH_3 + H \rightarrow C_2H_5$	75.9 (72.6)	−93.2 (−82.5)
Cu(111)	$C_2H_2 + H \rightarrow C_2H_3$	124.9 (125.0)	−27.8 (−28.6)
	$C_2H_3 + H \rightarrow C_2H_4$	86.4 (84.0)	−69.6 (−69.0)
	$C_2H_3 + H \rightarrow CHCH_3$	119.7 (126.0)	−18.1 (−19.6)
	$C_2H_4 + H \rightarrow C_2H_5$	114.0 (112.6)	−23.1 (−24.0)
	$CHCH_3 + H \rightarrow C_2H_5$	99.6 (93.4)	−74.6 (−73.4)
PdCu(111)	$C_2H_2 + H \rightarrow C_2H_3$	95.7(96.6)	−15.6(−13.8)
	$C_2H_3 + H \rightarrow C_2H_4$	71.2(70.1)	−73.6(−75.1)
	$C_2H_3 + H \rightarrow CHCH_3$	131.1(130.1)	−7.7(−7.7)
	$C_2H_4 + H \rightarrow C_2H_5$	146.6(145.3)	−20.6(−15.7)
	$CHCH_3 + H \rightarrow C_2H_5$	80.3(78.0)	−86.5(−83.1)

*it is noted that the values in parenthesis are obtained at 425 K.

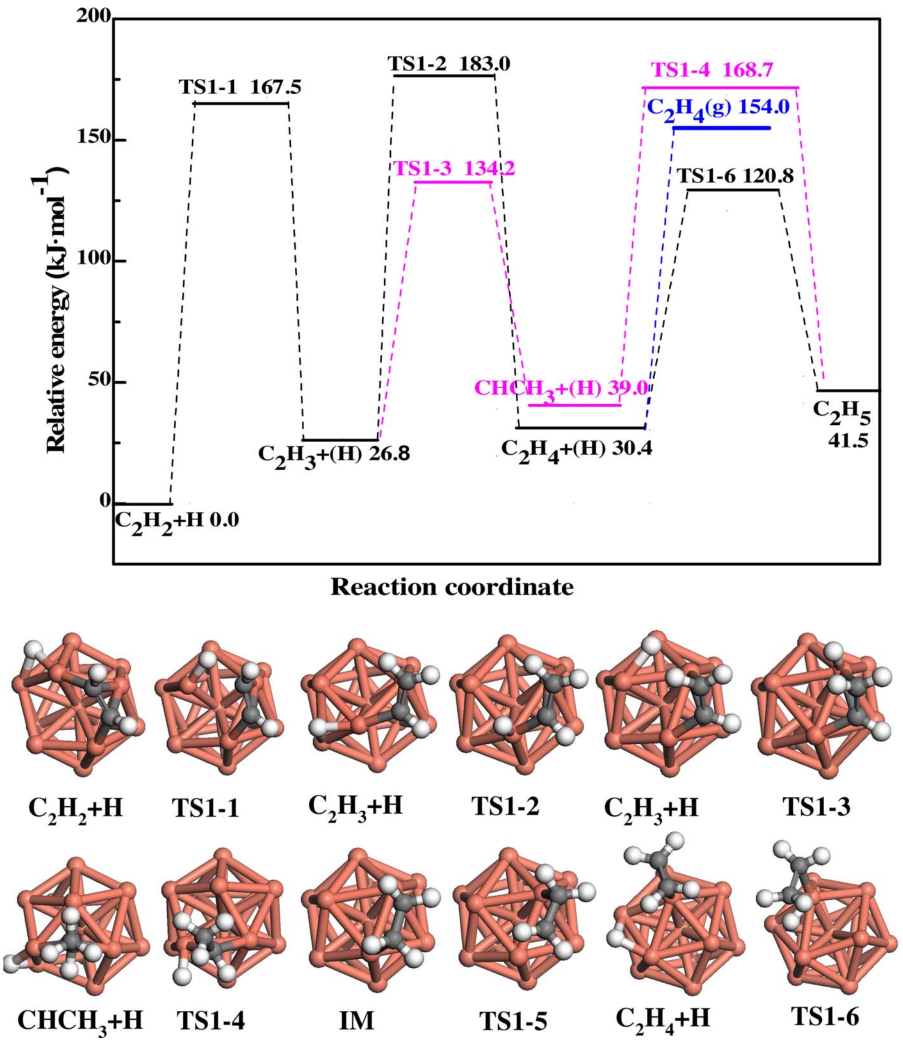

Fig. 4. Potential energy diagram for three pathways involving in C_2H_2 selective hydrogenation together with the structures of reactants and transition states on Cu_{13} cluster at 525 K.

has an activation barrier of 167.5 kJ mol^{-1} *via* the transition state TS1-1, it is endothermic by 26.8 kJ mol^{-1}. Starting from C_2H_3 intermediate, in Path I, C_2H_3 hydrogenation to C_2H_4 via TS1-2 needs a higher activation barrier of 156.2 kJ mol^{-1}, and it is endothermic by 3.6 kJ mol^{-1}, in this reaction, an intermediate IM (C_2H_4 species interacting with two Cu atoms via *di*–σ model) is formed, subsequently, it can be easily transferred to the favorable site with only a small activation barrier of 27.7 kJ mol^{-1}. Further, C_2H_4 desorb from the cluster surface with the desorption barrier of 133.6 kJ mol^{-1}.

In Path II, the first two steps to form C_2H_4 adsorbed at the cluster surface are similar to that in Path I, however, the formed C_2H_4 continues to hydrogenation to produce C_2H_5 *via* TS1-6, this elementary reaction has an activation barrier of 90.4 kJ mol^{-1}, and it is endothermic by 11.1 kJ mol^{-1}.

In Path III, starting from C_2H_3 intermediate, it goes through two hydrogenation steps to form C_2H_5 via another intermediate $CHCH_3$, the activation barriers of these two hydrogenation steps *via* TS1-3 and TS1-4 are 107.4 and 129.7 kJ mol^{-1} with reaction energies of 12.2 and 2.5 kJ mol^{-1}, respectively.

Since C_2H_3 is the common intermediate for three pathways, in order to identify the favorable pathway, the co-adsorbed C_2H_3 + H species is selected as the starting point, as shown in Fig. 4, it is clear that the highest barriers of three pathways are 183.0, 183.0 and 168.7 kJ mol^{-1}, respectively. Obviously, Path III is the most favorable pathway with C_2H_2 successive hydrogenations to form C_2H_5 *via* $CHCH_3$ intermediate. Moreover, C_2H_4 prefers to be hydrogenated to C_2H_5 rather than its desorption (90.4 *vs.* 133.6 kJ mol^{-1}).

Above result show that C_2H_2 selective hydrogenations to form C_2H_5 *via* $CHCH_3$ intermediate is the dominant pathway, namely, ethane is the major product rather than C_2H_4 on Cu_{13} cluster at 525 K. On the other hand, as shown in Fig. S7, the same result can be obtained when the reaction occurs at 425 K.

3.3.4. C_2H_2 hydrogenation on Cu_{38} cluster

As shown in Fig. 5, in Paths I and II, C_2H_4 prefers to be desorption to form gas phase C_2H_4 rather than being hydrogenated to form C_2H_5 (96.9 *vs.* 123.0 kJ mol^{-1}), suggesting that C_2H_2 can be selectively hydrogenated to form C_2H_4 via Path I. However, starting from C_2H_3 + H species, it is noted that for Path III with C_2H_2 successive hydrogenations to form C_2H_5 via $CHCH_3$ intermediate, the highest barrier is slightly smaller that of Path I (122.2 and 129.0 kJ mol^{-1}), which means that competitive relationship exists between these two pathways.

Thus, Path I to form C_2H_4 is energetically compatible with Path III to produce ethane in C_2H_2 selective hydrogenation, namely, the major products are ethane and ethylene on Cu_{38} cluster at 525 K. On the other hand, as presented in Fig. S8, the same result can be obtained when the reaction occurs at 425 K.

3.3.5. C_2H_2 hydrogenation on Cu_{55} cluster

As shown in Fig. 6, C_2H_4 prefers to desorption to form gas phase C_2H_4 in Path I rather than being hydrogenated to form C_2H_5 in Path II (115.6 *vs.* 124.8 kJ mol^{-1}), which means that C_2H_2 can be selectively hydrogenated to form gas phase C_2H_4 *via* Path I with the $\triangle E_a$ of 9.2 kJ mol^{-1}. Moreover, starting from C_2H_3 + H species, the highest

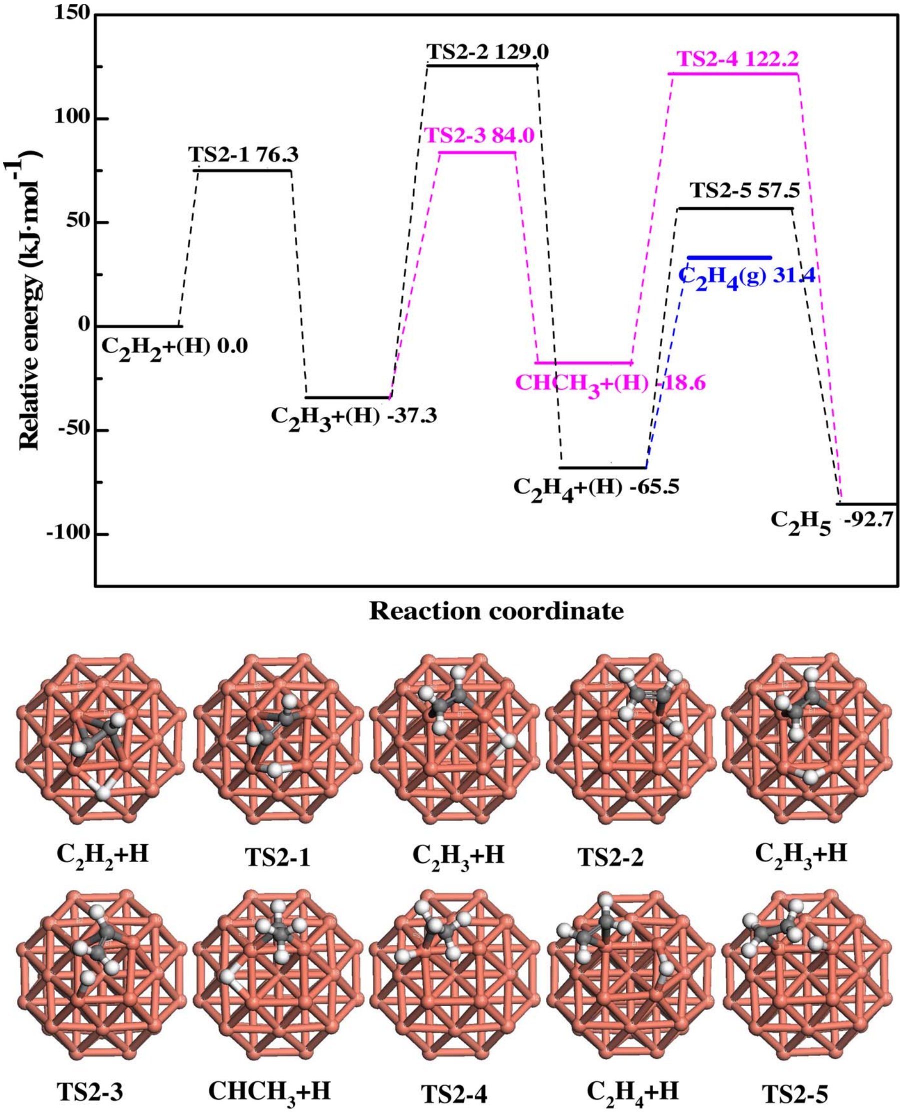

Fig. 5. Potential energy diagram for three pathways of C_2H_2 selective hydrogenation together with the structures of reactants and transition states on Cu_{38} cluster at 525 K.

barrier of Path I to form gas phase C_2H_4 is much smaller that of Path III to form C_2H_5 (81.7 and 130.3 kJ mol^{-1}).

Therefore, among three pathways, Path I to form gas phase C_2H_4 is the dominate pathway in C_2H_2 selective hydrogenation, namely, the major product is C_2H_4 on Cu_{55} cluster at 525 K. On the other hand, the same result can be obtained when the reaction occurs at 425 K, as seen in Fig. S9. Thus, Cu_{55} cluster at 525 and 425 K can effectively remove the small amount of C_2H_2 impurities in ethylene feed. The reaction rates of C_2H_4 formation are 2.56×10^{-1} and $1.01 \times 10^{-5} s^{-1}$ site^{-1} with the $\triangle E_a$ of 32.4 and 9.2 kJ mol^{-1} on 425 and 525 K, respectively, suggesting that the higher reaction temperature is in favor of the enhancement of the activity, however, it decrease the selectivity of C_2H_4 formation.

3.3.6. *C_2H_2 hydrogenation on Cu(111) surface*

As shown in Fig. 7, at 525 K, similar to Cu_{55} cluster, C_2H_4 prefers to be desorption to form gas phase C_2H_4 in Path I rather than being hydrogenated to form C_2H_5 in Path II (70.6 *vs.* 114.0 kJ mol^{-1}) with the $\triangle E_a$ of 43.4 kJ mol^{-1}. Moreover, starting from C_2H_3 + H species, the highest barrier of Path I to form gas phase C_2H_4 is also smaller that of Path III to form C_2H_5 (58.6 and 91.9 kJ mol^{-1}).

As a result, C_2H_4 is still the major product on Cu(111) surface at 525 K; the same result can be obtained at 425 K, as illustrated in Fig. S10. Namely, Cu(111) surface can exhibit the high selectivity towards gas phase C_2H_4 formation to removes the small amount of C_2H_2 impurities in ethylene feed. The reaction rates of C_2H_4 formation are 3.84×10^{-3} and $4.09 s^{-1}$ site^{-1} with the $\triangle E_a$ of 19.9 and 43.4 kJ mol^{-1} on 425 and 525 K, respectively, indicating that on Cu(111) surface, the higher reaction temperature is beneficial for the enhancement of the activity and the selectivity towards C_2H_4 formation, and can purify the acetylene-ethylene feed gas effectively.

3.4. *General discussion*

3.4.1. *The effect of Cu cluster size on the selectivity of C_2H_4 formation*

On the basis of above results, firstly, it is obvious that the size of Cu cluster can affect the adsorption behavior of C_2H_2 and C_2H_4 species; meanwhile, with the increasing of Cu cluster size, the adsorption energy of C_2H_4 decreases, which will beneficial to C_2H_4 desorption from Cu catalyst surface to form gas phase C_2H_4; moreover, the differences of adsorption energy between C_2H_2 and C_2H_4 species are always maintained at a high level (more than 40 kJ mol^{-1}), that is in favor of removing the small amount of C_2H_2 impurities from the larger amount of ethylene feed.

Secondly, the size of Cu cluster alters the most favorable pathway and major product of C_2H_2 selective hydrogenation. For Cu_{13} cluster, the most favorable pathway is C_2H_2 successive hydrogenations to form C_2H_5 *via* $CHCH_3$ intermediate, ethane is the major product. For Cu_{38}

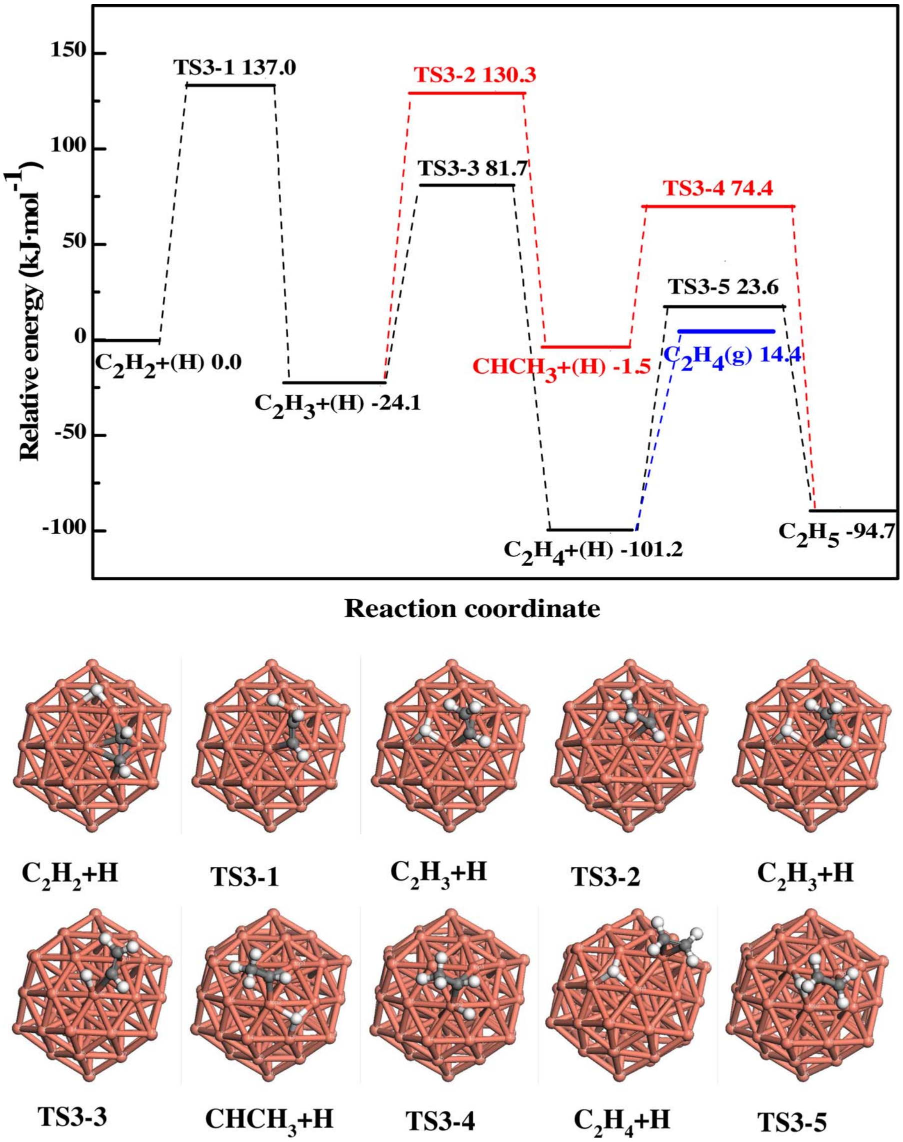

Fig. 6. Potential energy diagram for three pathways of C_2H_2 selective hydrogenation together with the structures of reactants and transition states on Cu_{55} cluster at 525 K.

cluster, two parallel pathways to form C_2H_4 and C_2H_5 are the most favorable pathways, namely, the major products are ethane and ethylene. For Cu_{55} cluster and the periodic Cu(111) surface regarded as the large size of Cu catalyst, the pathway to form gas phase C_2H_4 is the most favorable pathway, and the major product is C_2H_4, suggesting that the large size of Cu clusters can remove the small amount of C_2H_2 impurities in large amount of ethylene feed.

Further, in order to better understand the effect of Cu cluster size on the selectivity of C_2H_2 hydrogenation to C_2H_4, it is necessary to quantify the selectivity between C_2H_4 and ethane. Since ethane can be formed by C_2H_5 hydrogenation, and C_2H_3 is the common intermediates, starting from C_2H_3 + H species, Fig. 9 presents the comparisons of the simplified potential energy profile for the most favorable formation pathways of C_2H_4 and C_2H_5 on Cu_{13}, Cu_{38}, Cu_{55} clusters and Cu(111) surface, the selectivity is determined by the effective barrier difference between C_2H_4 and C_2H_5 formation [64]. In general, the higher barrier differences between C_2H_5 and C_2H_4 species formation means the higher selectivity towards C_2H_4 formation. The results show that starting from C_2H_3 + H species, the overall barrier differences between C_2H_5 and C_2H_4 are −14.3, −6.8, 48.6 and 33.3 kJ mol^{-1} on Cu_{13}, Cu_{38}, Cu_{55} clusters and Cu(111) surface, respectively; suggesting that ethane formation is more favorable kinetically than C_2H_4 on Cu_{13} and Cu_{38} clusters. However, C_2H_4 formation is more favorable kinetically than C_2H_5 on Cu_{55} cluster and Cu(111) surface, which exhibit a good selectivity towards C_2H_4 formation rather than ethane, and the size of Cu_{55} cluster has presented a similar catalytic performance with Cu bulk surface.

Above results show that the selectivity of gas phase C_2H_4 formation increases with the increasing of Cu cluster size. Starting from Cu_{55} cluster, Cu catalyst presents a good selectivity towards C_2H_4 formation rather than ethane compared to other small Cu clusters, the reason may be attributed to that the weaker adsorption ability of adsorbed species on Cu_{55} cluster and Cu(111) surface, especially for C_2H_4 species, becomes a thermodynamic driving force to lower the barrier of C_2H_4 desorption.

3.4.2. The effect of Cu cluster size on the activity of C_2H_4 formation

With the purpose of quantitatively describing the catalytic activity of gas phase C_2H_4 formation, a two-step model is employed to calculate the reaction rate, in which the coverage of the mentioned species is also considered. The detailed descriptions about two-step model have been systematically reported by Hu *et al.* [65,66], as presented in the Supplementary material.

The reaction rate is obtained by Eq. (7):

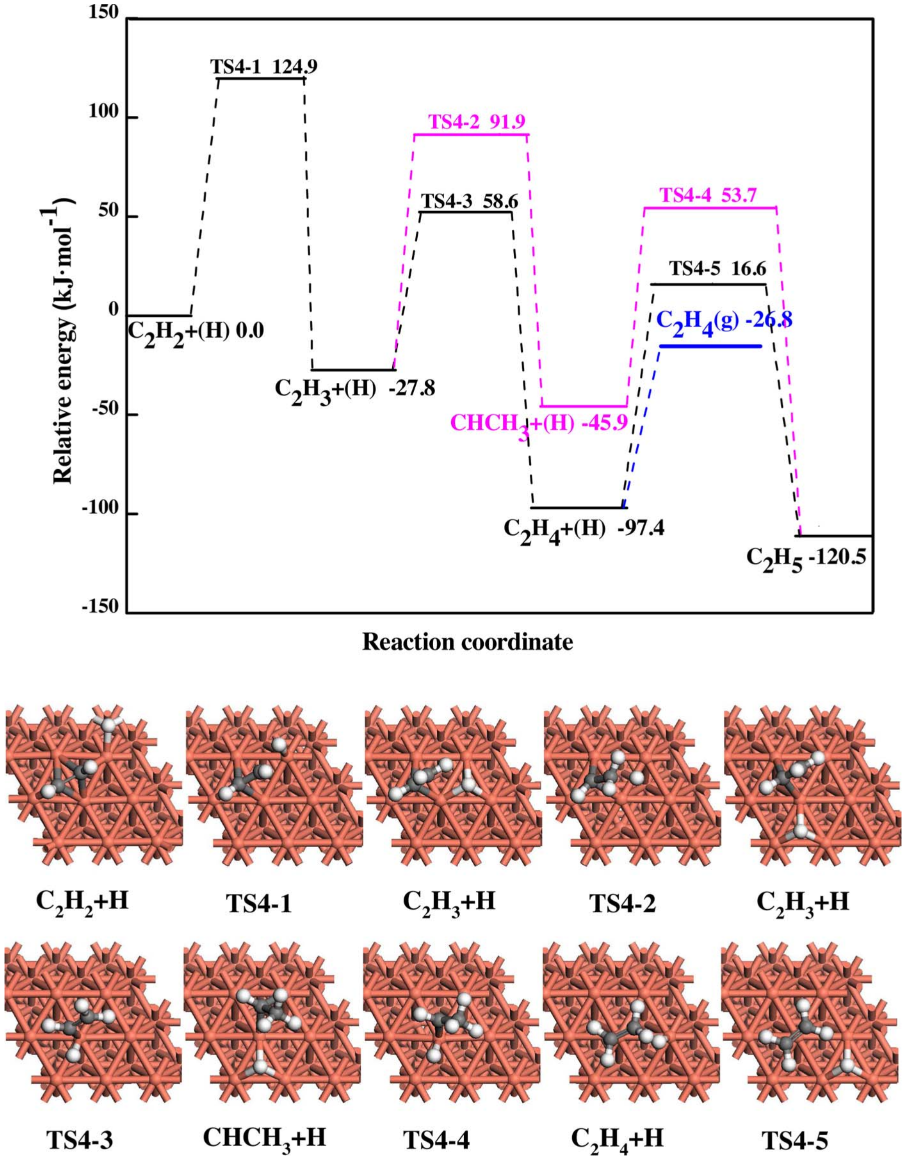

Fig. 7. Potential energy diagram for three pathways of C_2H_2 selective hydrogenation together with the structures of reactants and transition states on Cu(111) surface at 525 K.

$$r = \frac{K_B T}{h}\frac{\left(1-\frac{P_P}{P_R}e^{\frac{\Delta G}{RT}}\right)}{\frac{P^0}{P_R}e^{\frac{G_R^{ad}+G_R^{de}+G_P^{de}}{RT}}+e^{\frac{G_P^{de}}{RT}}} \tag{7}$$

Where k_b, h and R are constants, T, P_R and P_P represent the reaction temperature, partial pressure of reactants and products, respectively; G_R^{ad} and G_R^{de} are the effective free barriers of reactant adsorption and desorption, respectively. G_P^{de} is the effective free barrier of product desorption. ΔG is the free energy change of overall reaction at 525 and 425 K with the corresponding $\frac{kbT}{h} = 1.0938 \times 10^{13}$ and 8.8554×10^{12}, respectively; Thus, the overall reaction rate is dominantly related to *Gad R*, *Gde R* and *Gde P*.

Table 2
The values of $G_R^{ad} - G_R^{de} + G_P^{de}$, G_P^{de} (kJ mol^{-1}) and reaction rate (r/s^{-1} site^{-1}) at 525 and 425 K on Cu_{13}, Cu_{38}, Cu_{55} clusters, Cu(111) and PdCu(111) surface.

Clusters	$G_R^{ad} - G_R^{de} + G_P^{de}$	*Gde P*	*r*
Cu_{13}	−182.1(−189.8)	183.0(184.8)	6.78×10^{-6} (1.71×10^{-10})
Cu_{38}	−103.5(−84.8)	129.0(126.5)	1.60(2.51×10^{-3})
Cu_{55}	−78.5(−34.8)	137.0(146.0)	2.56×10^{-1}(1.01×10^{-5})
Cu(111)	−48.8(−33.2)	124.9(125.0)	4.09(3.84×10^{-3})
PdCu(111)	−104.4(−105.7)	95.7(96.6)	3.29×10^{3}(1.19×10^{1})

*it is noted that the values in parenthesis are obtained at 425 K.

The energetic terms in the denominator of Eq. (7) are listed in Table 2, we can see that *G*de P is much higher than G_R^{ad} - G_R^{de} + G_P^{de} on Cu_{13}, Cu_{38}, Cu_{55} clusters and Cu(111) surface, in which G_R^{ad} - G_R^{de} + G_P^{de} is negative, while G_P^{de} is positive, they all appear on index, which means that the effect of G_P^{de}on reaction rate is much larger than that of G_R^{ad} - G_R^{de} + G_P^{de}, as a result, G_P^{de} will be the effective barriers of C_2H_4 formation. Thus, according to the reaction rate, as listed in Table 2, the catalytic activity of gas phase C_2H_4 formation follows the order: Cu(111) > Cu_{38} > Cu_{55} > > Cu_{13}.

In order to reveal the microscopic reason of catalytic activity of C_2H_4 formation, the projected density of states (*p*DOS) and *d*-band analysis are conducted to provide a physical explanation. As we all know, as a key parameter, the *d*-band center is usually selected to measure the distribution of solid energy levels, and it can also reveal the ability to eject an electron to the adsorbed molecule from metal *d*-band. The *d*-band center is calculated as follows [67]:

$$\varepsilon_d = \frac{\int_{-\infty}^{E_f} E\rho_d(E)dE}{\int_{-\infty}^{E_f} \rho_d(E)dE} \tag{8}$$

Where ρ_d represents the density of states projected onto Cu atom's *d*-

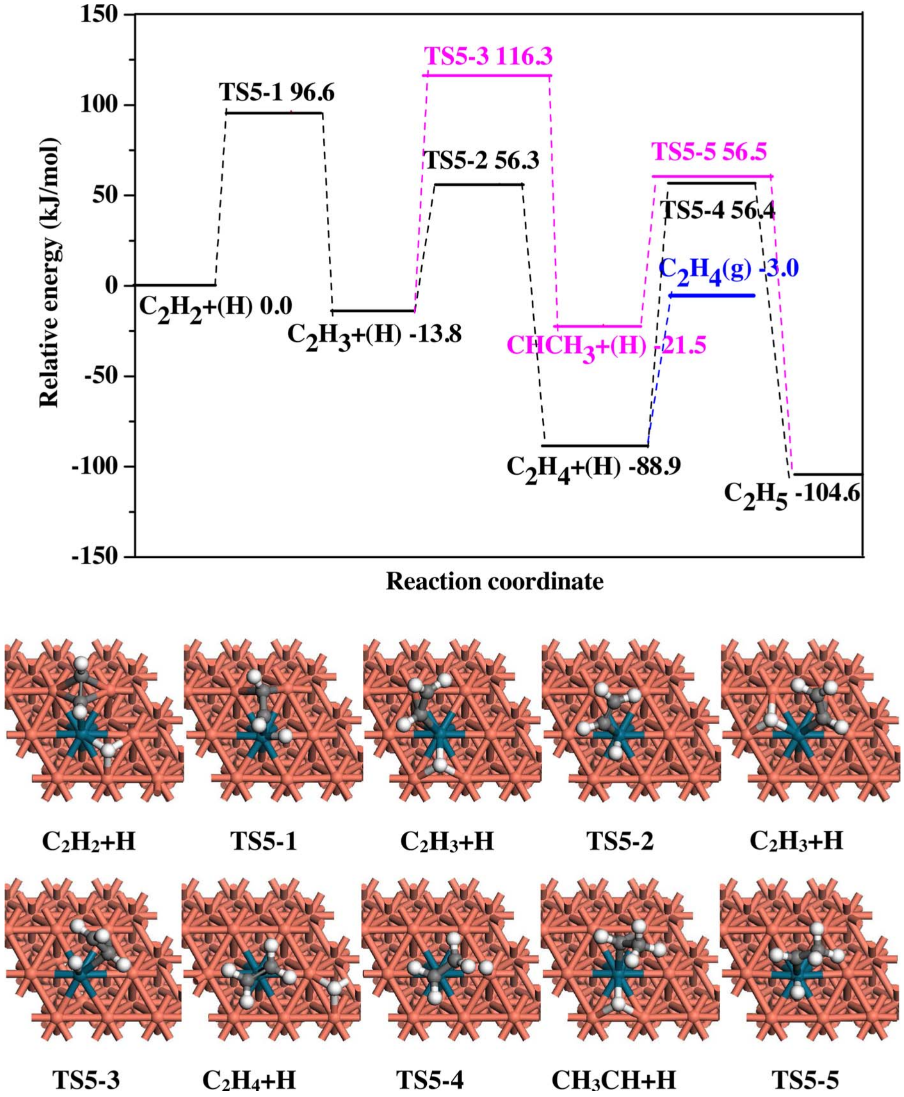

Fig. 8. Potential energy diagram for three pathways of C_2H_2 selective hydrogenation together with the structures of reactants and transition states on Pd-doped Cu(111) surface at 425 K.

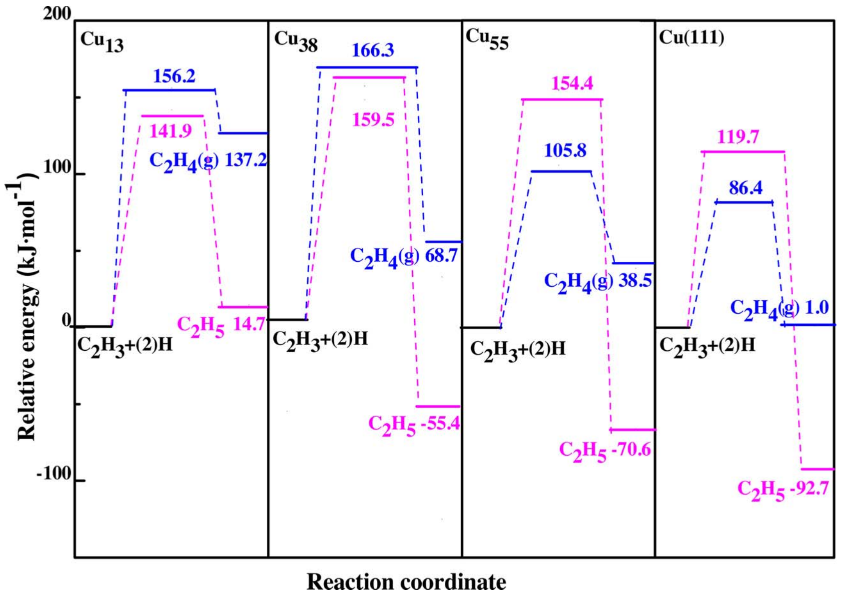

Fig. 9. The comparison of the simplified potential energy profile for the most favorable formation pathway of C_2H_4 and C_2H_5 on different Cu clusters and Cu(111) surface at 525 K, respectively.

band, and E_f is the Fermi energy.

For C_2H_x hydrogenation on Cu catalysts, since C_2H_x species interacts with Cu catalyst surface via C atoms, it is regarded as a process that H atom inserts into the Cu-C bond. The findings by Pallassana and Neurock on C_2H_4 hydrogenation suggest that the C—H bond activation of ethyl and ethylene is primarily guided by electron-back donation to the antibonding σCH* orbital, the catalytic activity of C—H bond formation increases on Pd catalyst surfaces where the *d*-band is far from the Fermi level [68,69], which also agree with the previous studies about CH_x hydrogenation to CH_4 [70–72]. Thus, the surface where the *d*-band center is far from the Fermi energy is more active for hydrogenation and the *d*-band center of outer layer Cu atoms on Cu clusters is selected to reveal the activity of C_2H_x hydrogenation.

As shown in Fig. 10, the *d*-band center (eV) of different clusters is $Cu_{13}(-2.09) > Cu_{55}(-2.25) > Cu(111)(-2.46) > Cu_{38}(-2.48)$, suggesting that Cu_{13} is the nearest to the Fermi energy level; both Cu_{38} cluster and Cu(111) surface are far from the Fermi energy level; the Fermi energy level of Cu_{55} cluster is located at medium range. As a result, the reaction rate (s^{-1} site^{-1}) of C_2H_4 formation is that Cu_{13} (6.78×10^{-6}) < Cu_{55} (2.56×10^{-1}) < Cu_{38} (1.60) < Cu(111) (4.09), in which the *d*-band center of Cu_{38} cluster is close to that of Cu(111) surface, and the reaction rate of Cu_{38} cluster and Cu(111) surface are also close. In general, for C_2H_2 hydrogenation to C_2H_4, when the *d*-band center of Cu catalyst is far away from the Fermi energy, Cu catalyst exhibits the higher catalytic activity towards C_2H_4 formation.

3.4.3. The effect of Pd-doped Cu(111) surface on C_2H_2 selective hydrogenation

Previous studies have shown that Pd-doped Cu-based bimetallic catalysts (PdCu bimetallic catalyst) are widely used in the selective hydrogenation of C_2H_2 [26,27,29,73], a very small quantity of Pd on Cu (111) surface can effectively promote the selective hydrogenation of C_2H_2 to C_2H_4, and exhibits a higher selectivity towards C_2H_4 formation than the pure Cu or Pd alone [26]. McCue et al. [27,73] also confirmed that Cu/Al_2O_3 catalysts modified with a small quantity of Pd also have a high selectivity and activity towards C_2H_4 formation in the selective hydrogenation of C_2H_2. However, few studies have investigated the underlying mechanism about the effect of promoter Pd on the selective hydrogenation of C_2H_2 over PdCu bimetallic catalysts. As a result, the selective hydrogenation of C_2H_2 over Pd-doped Cu(111) surface is further investigated.

As shown in Fig. 8, at 425 K, similar to Cu(111) surface (shown in Fig. S10), C_2H_4 prefers to be desorption to form gas phase C_2H_4 in Path I rather than being hydrogenated to form C_2H_5 in Path II (85.9 *vs.* 145.3 kJ mol^{-1}). Moreover, starting from C_2H_3 + H species, the highest barrier of Path I to form gas phase C_2H_4 is also smaller that of Path III to form C_2H_5 (56.3 *vs.* 116.3 kJ mol^{-1}). Meanwhile, for the selectivity towards C_2H_4 formation, the $\triangle E_a$ on Pd-doped Cu(111) surface is higher than that on Cu(111) surface (59.4 *vs.* 49.9 kJ mol^{-1}), suggesting that when the selective hydrogenation of C_2H_2 occurs over Pd-doped Cu catalyst, the selectivity of gas phase C_2H_4 formation increases. Thus, C_2H_4 is still the major product on Pd-doped Cu(111) surface, PdCu bimetallic catalyst can exhibit a high selectivity towards gas phase C_2H_4 formation than Cu catalyst alone, which is more favorable to remove the small amount of C_2H_2 impurities in ethylene feed. On the other hand, C_2H_4 desorption pathway has the highest barrier energy is 96.6 kJ mol^{-1} over Pd-doped Cu(111) surface, while it is 125.0 kJ mol^{-1} on Cu(111) surface. The reaction rates of gas phase C_2H_4 formation on Cu(111) and PdCu(111) are 3.84×10^{-3} and $1.19 \times 10^{1} s^{-1}$ site^{-1} at 425 K, respectively, suggesting that when the selective hydrogenation of C_2H_2 occurs over Pd-doped Cu catalyst, the activity of gas phase C_2H_4 formation significantly increases compared to Cu catalyst.

Therefore, when Pd is doped on Cu catalysts, compared to Cu catalyst, PdCu bimetallic catalyst can enhance the activity and selectivity of C_2H_4 formation, which is in agreement with the previous experimental results [26,27,73].

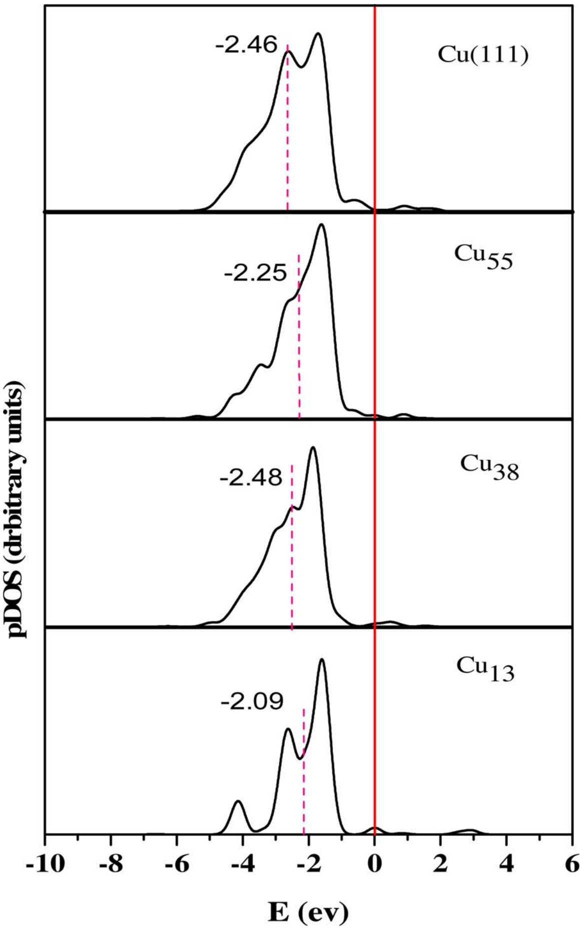

Fig. 10. Projected density of states (*p*DOS) plots of the *d*-orbitals for the outer layer Cu atoms of Cu clusters and Cu(111) surface. The vertical dashed lines represent the location of *d*-band center, and the vertical solid lines indicate Fermi energy level.

4. Conclusions

In this work, extensive DFT calculations have been carried out to examine the activity and selectivity of Cu catalyst towards C_2H_2 selective hydrogenation to C_2H_4, and to reveal the size effect of Cu catalyst on the activity and selectivity. Here, Cu_{13}, Cu_{38} and Cu_{55} nanoparticles with the corresponding diameters of 4.9, 7.6 and 9.8 Å are selected to model the different sizes of Cu catalyst, and the periodic Cu (111) surface is considered to represent the much larger particle. The results showed that the preferable pathway of C_2H_4 formation and the corresponding selectivity changes with the increasing of Cu catalyst size, in which ethane is the major product on Cu_{13} cluster, both ethane and ethylene is the major products on Cu_{38} cluster. However, the gas phase C_2H_4 becomes the major product on both Cu_{55} cluster and the periodic Cu(111) surface, suggesting that only the large size of Cu cluster can removes the small amount of C_2H_2 impurities from the large amount of ethylene feed. On the other hand, the catalytic activity of C_2H_2 hydrogenation to C_2H_4 has the relationship with the *d*-band center of Cu catalysts. Thus, the catalytic activity and selectivity of C_2H_2 hydrogenation to C_2H_4 is closely related to the size of Cu catalyst, in order to obtain the high activity and selectivity towards C_2H_4 formation, it is necessary to keep Cu catalysts at a relatively larger size level in the industrial applications.

Acknowledgments

This work is financially supported by the National Natural Science Foundation of China (No. 21776193, 21476155), the China Scholarship Council, the Program for the Top Young Academic Leaders of Higher Learning Institutions of Shanxi, and the Top Young Innovative Talents of Shanxi.

Appendix A. Supplementary data

Supplementary data associated with this article can be found, in the online version, at http://dx.doi.org/10.1016/j.apcata.2017.08.001.

References

[1] A. Borodzin´ski, G.C. Bond, Catal. Rev.: Sci. Eng. 48 (2006) 91–144.
[2] A. Borodzin´ski, G.C. Bond, Catal. Rev.: Sci. Eng. 50 (2008) 379–469.
[3] L.D. Shao, B.S. Zhang, W. Zhang, D. Teschner, F. Girgsdies, R. Schlögl, D.S. Su, Chem. Eur. J. 18 (2012) 14962–14966.
[4] N.A. Khan, S. Shaikhutdinov, H.J. Freund, Catal. Lett. 108 (2005) 159–164.
[5] J. Sá, G.D. Arteaga, R.D. Daley, J. Bernardi, J.A. Anderson, J. Phys. Chem. B 110 (2006) 17090–17095.
[6] D. Teschner, J. Borsodi, A. Wootsch, Z. Revay, M. Kaveckre, A. Knop-Gericke, S.D. Jackson, R. Schlögl, Sci 320 (2008) 86–89.
[7] H. Gabasch, K. Hayek, A. Knop-Gericke, R. Schlögl, J. Phys. Chem. B 110 (2006) 4947–4952.
[8] M. García-Mota, B. Bridier, J. Pérez-Ramírez, N. López, J. Catal. 273 (2010) 92–102.
[9] F.M. McKenna, J.A. Anderson, J. Catal. 281 (2011) 231–240.
[10] A.J. McCue, F.M. McKenna, J.A. Anderson, Catal. Sci. Technol. 5 (2015) 2449–2459.
[11] B. Bridier, N. López, J. Pérez-Ramírez, Dalton Trans. 39 (2010) 8412–8419.
[12] M. Armbruster, M. Behrens, F. Cinquini, K. Föttinger, Y. Grin, A. Haghofer, B. Klötzer, A. Knop-Gericke, H. Lorenz, A. Ota, S. Penner, J. Prinz, C. Rameshan, Z. Révay, D. Rosenthal, G. Rupprechter, D. Teschner, D. Torres, R. Wagner, R. Widmer, G. Wowsnick, Chem. Cat. Chem. 4 (2012) 1048–1063.
[13] S. Schauermann, N. Nilius, S. Shaikhutdinov, H.J. Freund, Acc. Chem. Res. 46 (2013) 1673–1681.
[14] W. Ludwig, A. Savara, K.H. Dosert, S. Shauermann, J. Catal. 284 (2011) 148–156.
[15] W. Ludwig, A. Savara, R.J. Madix, S. Schauermann, H.J. Freund, J. Phys. Chem. C 116 (2012) 3539–3544.
[16] M. Wilde, K. Fukutani, W. Ludwig, B. Brandt, J.H. Fischer, S. Schauermann, H.J. Freund, Angew. Chem. Int. Ed. 47 (2008) 9289–9293.
[17] J.T. Wehrli, D.J. Thomas, M.S. Wainwright, D.L. Trimm, Appl. Catal. 66 (1990) 199–208.
[18] J.T. Wehrli, D.J. Thomas, M.S. Wainwright, D.L. Trimm, Appl. Catal. 70 (1991) 253–262.
[19] N.J. Ossipoff, N.W. Cant, J. Catal. 148 (1994) 125–133.
[20] B. Bridier, N. López, J. Pérez-Ramírez, J. Catal. 269 (2010) 80–92.
[21] B. Bridier, M.A.G. Hevia, N. López, J. Pérez-Ramírez, J. Catal. 278 (2011) 167–172.
[22] E. Bus, J.T. Miller, J.A. van Bokhoven, J. Phys. Chem. B 109 (2005) 14581–14587.
[23] Y. Segura, N. López, J. Pérez-Ramírez, J. Catal. 247 (2007) 383–386.
[24] S.A. Nikolaev, V.V. Smirnov, Catal. Today 147 (2009) S336–S341.
[25] J. Jia, K. Haraki, J.N. Kondo, K. Domen, K. Tamaru, J. Phys. Chem. B 104 (2000) 11153–11156.
[26] G. Kyriakou, M.B. Boucher, A.D. Jewell, E.A. Lewis, T.J. Lawton, A.E. Baber, H.L. Tierney, M. Flytzani-Stephanopoulos, E.C. Sykes, Science 335 (2012) 1209–1212.
[27] Alan J. McCue, Callum J. McRitchie, Ashley M. Shepherd, J.A. Anderson, J. Catal. 319 (2014) 127–135.
[28] B. Bridier, J. Pérez-Ramírez, J. Am. Chem. Soc. 132 (2010) 4321–4327.
[29] F. Studt, F. Abild-Pedersen, T. Bligaard, R.Z. Sørensen, C.H. Christensen, J.K. Nørskov, Angew. Chem. Int. Ed. 47 (2008) 9299–9302.
[30] Z.J. Zuo, L. Wang, P.D. Han, W. Huang, Comput. Theor. Chem. 1033 (2014) 14–22.
[31] B. Delley, J. Chem. Phys. 113 (2000) 7756–7764.
[32] B. Delley, J. Chem. Phys. 92 (1990) 508–517.
[33] D.X. Tian, H.L. Zhang, J.J. Zhao, Solid State Commun. 144 (2007) 174–179.
[34] C.G. Zhou, J.P. Wu, A. Nie, F.R. C, A. Tachibana, H.S. Cheng, J. Phys. Chem. C 111 (2007) 12773–12778.
[35] T.A. Halgren, W.N. Lipscomb, Chem. Phys. Lett. 49 (1977) 225–232.
[36] N. Govind, M. Petersen, G. Fitzgerald, D. King-Smith, J. Andzelm, Comput. Mater. Sci. 28 (2003) 250–258.
[37] J. Greeley, M. Mavrikakis, Surf. Sci. 540 (2003) 215–229.
[38] G.C. Bond, R.S. Mann, J. Chem. Soc. (1959) 3566–3573.
[39] J.W. Lee, X.Y. Liu, C.Y. Mou, J. Chin. Chem. Soc. 60 (2013) 907–914.
[40] K. Shin, D.H. Kim, S.C. Yeo, H.M. Lee, Catal. Today 185 (2012) 94–98.
[41] W.Y. Li, F.Y. Chen, J. Nanopart. Res. 15 (2013) 1–14.
[42] Ş. Erkoç, R. Shaltaf, Phys. Rev. A 60 (1999) 3053–3057.
[43] M. Kabir, A. Mookerjee, A.K. Bhattacharya, Phys. Rev. A 69 (2004) (043203-1-10).
[44] J.P.K. Doye, D.J. Wales, New J. Chem. 22 (1998) 733–744.
[45] S. Darby, T.V. Mortimer-Jones, R.L. Johnston, C. Roberts, J. Chem. Phys. 116 (2002) 1536–1550.
[46] S. Özçelik, Z.B. Güvenç, Surf. Sci. 532 (2003) 312–316.
[47] E. Fernández, M. Boronat, A. Corma, J. Phys. Chem. C 119 (2015) 19832–19846.
[48] S. Nunez, R.L. Johnston, J. Phys. Chem. C 114 (2010) 13255–13266.
[49] Y.H. Park, I.A. Hijazi, Mol. Simulat. 38 (2012) 241–247.
[50] R. Ferrando, A. Fortunelli, G. Rossi, Phys. Rev. B 72 (2005) 085449.
[51] I.A. Hijazi, Y.H. Park, Eur. Phys. J. D 59 (2010) 215–221.
[52] M. Itoh, V. Kumar, T. Adschiri, Y. Kawazoe, J. Chem. Phys. 131 (2009) 174510.
[53] H.F. Gong, W. Lu, L.M. Wang, G.P. Li, S.X. Zhang, Comput. Mater. Sci. 65 (2012) 230–234.
[54] H.F. Gong, W. Lu, L.M. Wang, G.P. Li, Chin. Phys. B 21 (2012) 190–197.
[55] L. Zhang, W. Li, Comput. Mat. Sci. 51 (2012) 91–95.
[56] U. Lammers, G. Borstel, Phys. Rev. B 49 (1994) 17360–17377.
[57] D. Liu, Y.F. Zhu, Q. Jiang, J. Phys. Chem. C 113 (2009) 10907–10912.
[58] L.E. Sutton (Ed.), Tables of Interatomic Distances and Configuration in Molecules and Ions, The Chemical Society, Burlington House, London, 1965.
[59] W. Liu, J.S. Lian, Q. Jiang, J. Phys. Chem. C 111 (2007) 18189–18194.
[60] B. Yang, R. Burch, C. Hardacre, G. Headdock, P. Hu, ACS Catal. 2 (2012) 1027–1032.
[61] B. Yang, R. Burch, C. Hardacre, G. Headdock, P. Hu, J. Catal. 305 (2013) 264–276.
[62] J.F. Paul, P. Sautet, J. Phys. Chem. 98 (1994) 10906–10912.
[63] X.M. Cao, R. Burch, C. Hardacre, P. Hu, Catal. Today 165 (2011) 71–79.
[64] T.H. Pham, Y.Y. Qi, J. Yang, X.Z. Duan, G. Qian, X.G. Zhou, D. Chen, W.K. Yuan, ACS Catal. 5 (2015) 2203–2208.
[65] J. Cheng, P. Hu, P. Ellis, S. French, G. Kelly, C.M. Lok, J. Phys. Chem. C 112 (2008) 1308–1311.
[66] J. Cheng, P. Hu, Angew. Chem. Int. Ed. 50 (2011) 7650–7654.
[67] S.D. Miller, J.R. Kitchin, Surf. Sci. 603 (2009) 794–801.
[68] R.A.V. Santen, M. Neurock, Molecular Heterogeneous Catalysis, Wiley-VCH, 2006.
[69] V. Pallassana, M. Neurock, J. Catal. 191 (2000) 301–317.
[70] C.F. Huo, Y.W. Li, J.G. Wang, H.J. Jiao, J. Am. Chem. Soc. 131 (2009) 14713–14721.
[71] T.H. Pham, Y.Y. Qi, J. Yang, X.Z. Duan, G. Qian, X.G. Zhou, D. Chen, W.K. Yuan, ACS Catal. 5 (2015) 2203–2208.
[72] J.D. Li, E. Croiset, R.S. Luis, J. Mol. Catal. A: Chem. 365 (2012) 103–114.
[73] A.J. McCue, A.M. Shepherd, J.A. Anderson, Catal. Sci. Technol. 5 (2015) 2880–2890.